Anal Bioanal Chem (2009) 393:1923–1929
DOI 10.1007/s00216-009-2638-7

ORIGINAL PAPER

Application of TEM and XPS in the interpretation of the kinetics of deuterium evolution from ultrathin TiD_y/Pd films evaporated on quartz

W. Lisowski · E. G. Keim

Received: 23 November 2008 / Revised: 18 January 2009 / Accepted: 20 January 2009 / Published online: 10 February 2009

Abstract The kinetics of thermal evolution of deuterium from ultrathin TiD_y/Pd bilayer films has been studied by means of thermal desorption mass spectrometry (TDMS). Using a combination of transmission electron microscopy (TEM) and X-ray photoelectron spectroscopy, we made a study of the complex structural and chemical transformations of the TiD_y/Pd film as a result of TDMS-induced evolution of deuterium and simultaneous annealing of this film. Both preparation and TDMS processing of the TiD_y/Pd bilayer films were performed in situ under UHV conditions. It was found that the high-temperature TDMS processing of an ultrathin TiD_y/Pd film, which was carried out in a relatively short time, leads to a significant film structure transformation. Energy-filtered TEM mapping of cross-section images and EDX analysis revealed extensive interdiffusion of Ti and Pd within the Ti–Pd bi-layer film. This process leads to a progressive change in chemical composition within the surface and subsurface area of the film during the TDMS processing. As the temperature of TDMS heating increases, segregation of Ti at the Pd top layer surface becomes significant. As a result, the kinetics of deuterium desorption is progressively changed during TDMS; at lower temperatures, the kinetics is limited by recombinative processes at the Pd surface, at temperatures beyond 500 K, it becomes dominated by interdiffusion of Ti into the Pd surface.

W. Lisowski (✉)
Institute of Physical Chemistry, Polish Academy of Sciences,
Kasprzaka 44/52,
01-224 Warsaw, Poland
e-mail: wlis@ichf.edu.pl

E. G. Keim (✉)
MESA+ Research Institute, NanoLab, Materials Characterization,
University of Twente,
P.O. Box 217, 7500 AE Enschede, The Netherlands
e-mail: e.g.keim@utwente.nl

Keywords Palladium · Titanium deuteride · SEM · TEM · XPS

Introduction

Thin TiD_y/Pd bilayer films can be applied as a useful source of deuterium used in chemical and energetic reactions [1–3]. Evolution of hydrogen from such material is realized at elevated temperatures, and this process can be monitored using the method of thermal desorption mass spectrometry (TDMS) [4]. In our previously published papers [5, 6], we presented the results of an extensive structural and chemical characterization of 100–200-nm-thick titanium deuteride films protected by a 10–12-nm-thick Pd layer against destructive air interaction. However, the results of our most recent studies related to titanium deuterated films [4], and the results reported by other authors [7, 8] revealed an essential role of the thickness-dependent morphology of the Ti film in the formation of a titanium deuteride (TiD_y) film and its subsequent decomposition. TDMS heating induced decomposition of fine-grained thin TiD_y films of 10–20 nm thickness proceeds at much lower temperature, and its kinetics is dominated by a lower energy desorption of deuterium as compared with the corresponding thick films. This observation stimulated our interest in the practical application of such films covered by a protective Pd layer as deuterium storage material. It is expected that TDMS processing of such TiD_y/Pd films will lead to a rearrangement of the bulk and surface morphology as a result of high-temperature annealing and simultaneous decomposition of the titanium deuteride. Therefore, a structural and chemical characterization of such ultrathin TiD_y/Pd films after thermal deuterium evolution is highly desirable. In this paper, we want to focus on three important points: (1) if the Pd top

layer affects the course of the TDMS controlled deuterium evolution from ultrathin TiD_y films, (2) what the tendency will be of the structural changes of the ultrathin TiD_y/Pd film as a result of TDMS processing, and (3) if the TDMS heating induced structural rearrangement of the Ti/Pd bilayer film would also affect the course of deuterium evolution from this film. In order to elucidate these points, we carried out a set of TDMS experiments in situ in the glass UHV system in which the films were prepared. An experimental investigation of selected samples was performed using transmission electron microscopy (TEM)—in combination with energy-filtered TEM (EFTEM) and energy dispersive X-ray spectrometry (EDX) —and X-ray photoelectron spectroscopy (XPS). A comparative study of the TiD_y/Pd films, before and after TDMS processing, was performed.

Experimental

Thin TiD_y/Pd films were prepared within a glass UHV system [9] using the following procedure: 10–12-nm-thick Ti films were evaporated onto a quartz substrate kept at 273 K at a pressure $\leq 1\times10^{-7}$ Pa. After evaporation, the films were annealed for 60 min at 650 K; the TiD_y films were then prepared by volumetrically controlled D_2 sorption at 298 K [10] until an equilibrium pressure of approx. 1 Pa was reached. After adsorption, deuterium was evacuated to the final steady pressure approaching 10^{-4} Pa, at which the TDMS was activated. Selected deuterated Ti films were covered in situ, prior to TDMS, by evaporation of a 10–12-nm-thick Pd layer.

Deuterium evolution as a result of annealing the TiD_y/Pd films was monitored in situ by TDMS [4]. The amount of deuterium absorbed within the titanium film was determined in this work by means of the volumetric method and compared with TDMS calculations [11]. Using the well-known mass of the Ti film and the deuterium uptake, we could estimate an average atomic ratio D/Ti for the investigated TiD_y/Pd films.

Morphological examination of the TiD_y/Pd films before and after TDMS processing was performed ex situ in separate analytical systems. Preparation of all films was, however, performed in a glass UHV apparatus at the same conditions as in the TDMS experiment. Each time thin Ti films were deposited onto a clean, quartz substrate plate (5 mm×8 mm in size and 1 mm thick), placed within the glass TDMS cell. The preparation procedure preceding TDMS was subsequently repeated in situ each time for a new sample. In this way, we were able to prepare specimens representative of the TiD_y/Pd films prior to TDMS and the corresponding films after the TDMS processing, respectively.

TEM analyses were carried out in a Philips CM300ST-FEG, which was equipped with a Gatan Tridiem energy filter and Thermo Fisher Noran System Six EDX analyzer with nanotrace EDX detector. The TEM specimens of the analyzed films were prepared in cross-section (XS) according to the recipe described in Ref. [12]. XSTEM images were used to extract information regarding the bulk structure of the corresponding films, whereas EFTEM analysis revealed the bulk element distribution in these films. The three-window method was used for the EFTEM analysis in order to minimize interference from Ti by Pd, vice versa. Verification of the correctness of the resulting Pd and Ti maps was provided by EDX analyses using a focused probe, as well as EFTEM Spectrum Imaging.

Additional chemical characterization of the annealed TiD_y/Pd films has been carried out using XPS [13]. The XPS spectra were recorded in a VG Scientific ESCALAB-210 spectrometer using Al Kα radiation (1486.6 eV) from an X-ray source operating at 15 kV and 20 mA. The spectra were collected with analyzer pass energy 20 eV, step size 0.1 eV, and at electron take-off angles of 90° and 20° relative to the surface plane. Shirley background subtraction and peak fitting with Gaussian–Lorentzian-shaped profiles was performed using Casa XPS software. The photoelectron peaks considered were Pd 3d and Ti 2p.

Results and discussion

Thermal desorption measurements

Figure 1 shows the TDMS spectra for deuterium from a thin deuterated titanium film (curve 1) and from a Ti film of similar thickness, which was exposed to deuterium under similar conditions and covered subsequently in situ by a Pd layer (curve 2). The TDMS spectra from both films were recorded under identical experimental conditions. The spectra reveal that deuterium evolution from thin TiD_y and TiD_y/Pd films is realized within a similar temperature range. However, the observed maximum peak temperature, T_m, of the spectrum taken from the TiD_y/Pd film is shifted by about 20 K to lower temperatures, and the amount of deuterium evolved from this film is approx. 30% lower than that of the TiD_y film. The average atomic ratio D/Ti determined by means of the volumetric method for TiD_y and TiD_y/Pd films prior to evaporation of the Pd top layer was found to be similar, i.e., 1.20±0.05 and agree well with the corresponding data, which we reported for the TiD_y films of similar thickness [4]. This result is strongly in favor of the idea that part of the deuterium was desorbed from the TiD_y film during post-evaporation of the Pd layer. Furthermore, the asymmetric shape of the TDMS spectra suggests a complex course of deuterium evolution from the TiD_y/Pd film. TEM and XPS analysis provided a clue regarding the origin of this process.

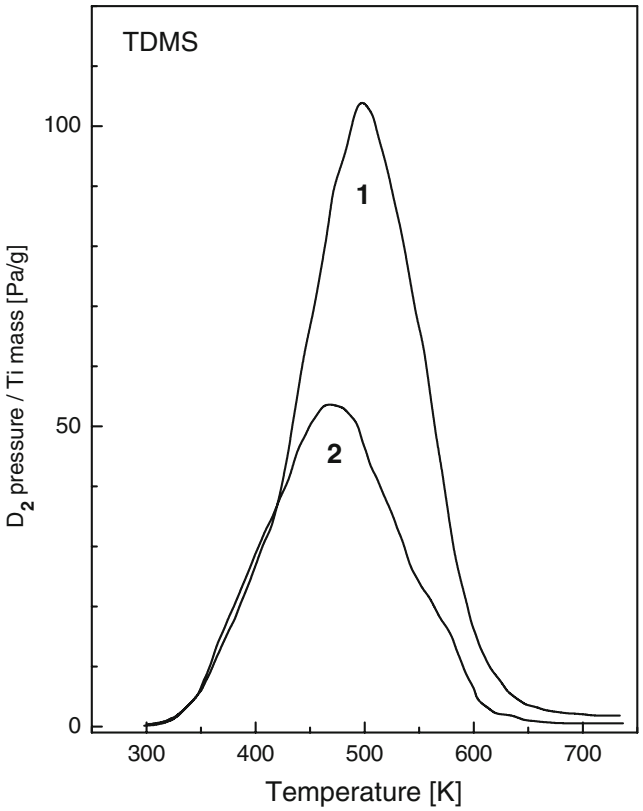

Fig. 1 Thermal desorption spectra of deuterium from ultrathin titanium deuterated films: as received (*curve 1*) and covered in situ prior to TDMS by a 10-nm-thick Pd layer (*curve 2*). Both titanium deuterated films were prepared under identical experimental conditions

Cross-sectional TEM analysis

Figure 2 shows the bright field (BF) TEM cross-sectional images of an ultrathin TiD_y/Pd film, recorded before (a) and after TDMS processing (b). The TEM image (a) shows distinct, sharp, and well-separated areas of the TiD_y and Pd layers in the TiD_y/Pd film before TDMS. Both the TiD_y and Pd layers exhibit a disordered bulk morphology, which is dominated by amorphous areas in addition to fine polycrystalline grains (8 – 12 nm). In contrast, intermixed areas of Ti and Pd layers forming the amorphous bulk structure morphology resulted after TDMS processing.

In Fig. 3, the results of the EFTEM analyses on the cross-section planes of the TiD_y/Pd film taken before (left column) and after (right column) TDMS processing are presented. In these columns, the BFTEM images, together with the associated EFTEM elemental mappings of Si ($L_{2,3}$ edge), Ti ($L_{2,3}$ edge), and Pd ($M_{4,5}$ edge), are compared. The elemental distribution is marked in white color (an area with bright intensity represents a higher elemental concentration than an area with dark intensity). To visualize the elemental distribution even more clearly, the elemental maps are combined into an RGB composite image presented in Fig. 4. In this figure, each elemental map of Si, Ti, and Pd is associated with a color, i.e., blue, green, and red, respectively.

Analysis of the EFTEM images reveals that an extensive intermixing process between the Ti and Pd layers occurs as a result of the TDMS processing. One can observe also a visible enrichment of Ti at the top of the surface of the Pd film (Figs. 3 and 4). The range of Pd and Ti atom penetration within the Ti/Pd interlayer area can be estimated from the EFTEM mapping images to be roughly 5–7 nm.

In order to verify this value, we can analyze the interdiffusion process of Ti and Pd atoms in the experimental conditions determined by the TDMS annealing. To consider this point, we can estimate a length of diffusion zone (L_{diff}) for Ti and Pd within the Pd–Ti interface using a simple relation of $\tau_{\mathrm{diff}}=(L_{\mathrm{diff}})^2/D_{\mathrm{diff}}$, where D_{diff} is a diffusion coefficient determined for each metal at the

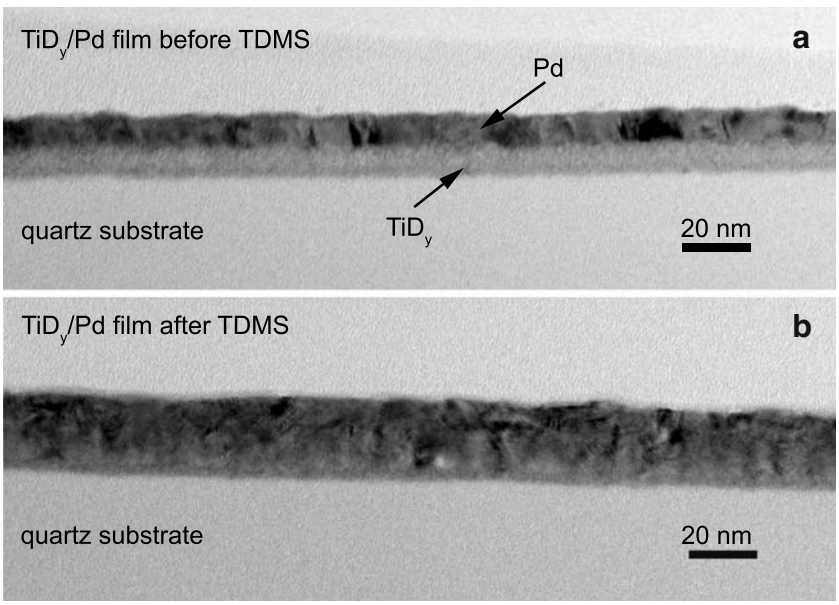

Fig. 2 Bright field cross-sectional TEM images of an ultrathin TiD_y/Pd film before (**a**) and after TDMS (**b**) processing

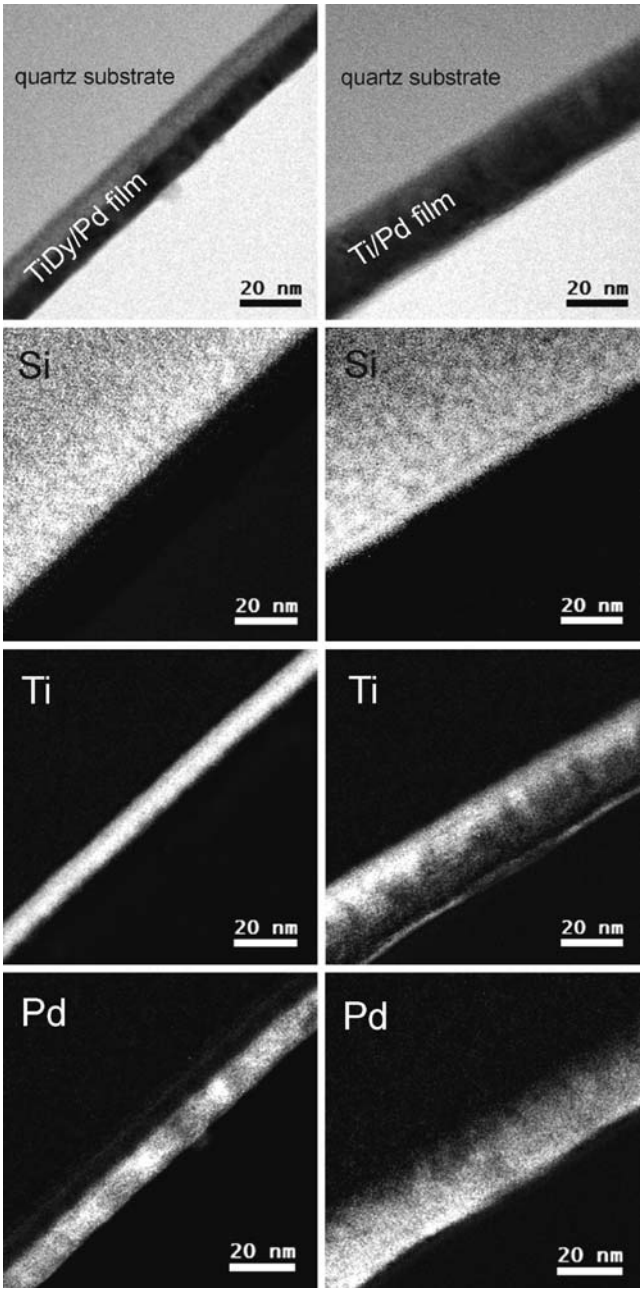

Fig. 3 EFTEM analysis of the TiD_y/Pd layer before (*left column*) and after TDMS processing (*right column*). The bright field cross-sectional XSTEM images of both films are presented on *top of each column*. Below the XSTEM images are shown the associated elemental mappings of Si ($L_{2,3}$ edge), Ti ($L_{2,3}$ edge), and Pd ($M_{4,5}$ edge). The elemental distribution is *marked in white color*

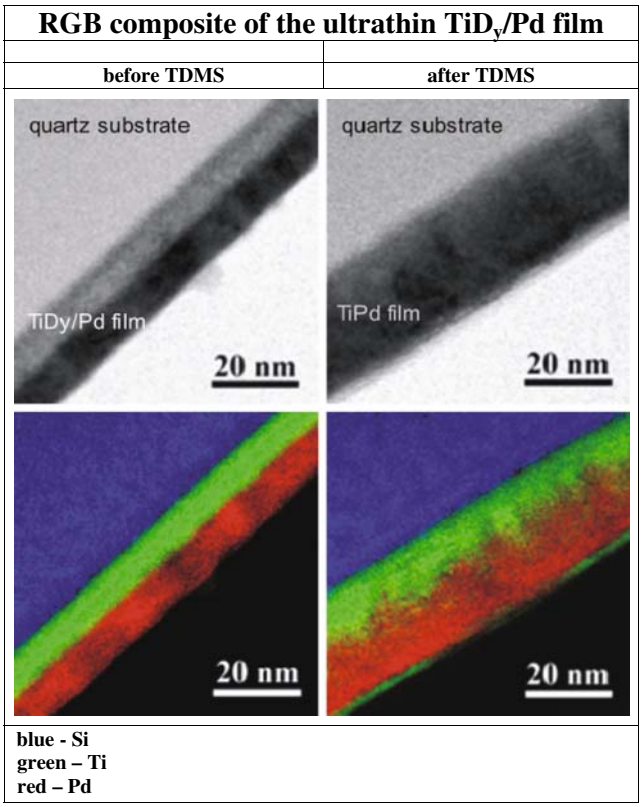

Fig. 4 RGB images of the ultrathin TiD_y/Pd film taken before and after TDMS. The bright field cross-sectional XSTEM images of both films are repeated from Fig. 3 and are presented on *top of each column*. Below the RGB images created by superimposing the elemental EFTEM maps of Si (*blue*), Ti (*green*), and Pd (*red*) are shown

annealing temperature and τ_{diff} is annealing time. Unfortunately, the annealing temperature is not constant in the whole TDMS process resulting in a relative increase of D_{diff} during thermal desorption. However, knowing the course of the simultaneously recorded parameters in TDMS, $P(D_2)$ versus time (t) and temperature (T) versus t, we can correlate in time the evolution of deuterium and film temperature increase. Thus, for each subsequent period of TDMS (dt), which is in fact part of the annealing time, we can estimate the average values for temperature (T_{av}) and D_{diff} (T_{av}). L_{diff} can be approximated in this case by:

$$L_{diff} = \left[\sum D_{diff}(T_{av})dt\right]^{1/2}. \quad (1)$$

Taking the literature values of the interdiffusion parameters for Pd and Ti, for diffusion in Pd–Ti bi-layer films (Table 1), we estimated D_{diff} (T_{av}) values for Pd and Ti in the temperature range determined by the TDMS process (see Fig. 5a), and then, using Eq. 1, the L_{diff} values for Pd and Ti were estimated at each following step of TDMS heating. The results of these calculations are presented in Fig. 5b. The final L_{diff} values at the end of TDMS were found to be to 5.0 and 5.5 nm, respectively, for the Ti and Pd diffusion zone. The estimated L_{diff} values are in good agreement with our EFTEM results.

The EFTEM mapping image of Ti reveals also a visible and significant enrichment of Ti at the top of the surface of the Pd film: In the right columns of Fig. 3 and Fig. 4, one can observe a very thin highly concentrated Ti layer (about 2 nm thick) on the top of the film assembly, which is

Table 1 Interdiffusion parameters of Pd and Ti in Pd/Ti systems

Diffusion system	D_0 [m^2 s^{-1}]	E_{diff} [eV]	T [K]	Ref.
Pd in α-Ti	$(2.0\pm0.5)\times10^{-3}$	2.74	723–1073	[14]
Pd in Pd/Ti film	$(1.0\pm0.3)\times10^{-14}$	0.78	523–623	[15]
Ti in Pd/Ti film	$(1.6\pm0.5)\times10^{-13}$	0.95	523–623	[15]

The values of activation energies (E_{diff}) and frequency factors (D_0), estimated at the temperature range T, are presented [14, 15]

separated by a dominant Pd layer that extends further into the deeper part of the Ti phase. Such an extensive surface segregation of Ti was not observed for annealed 100-nm-thick TiD_y films covered by a Pd layer of similar thickness [6]. These results strongly suggest that differences in bulk morphology are causing the observed different structural rearrangement paths accompanying decomposition of the deuteride phases in the films investigated. The thick TiD_y films are constituted mainly by a crystalline phase of relatively stable TiD_2, which decomposed at much higher

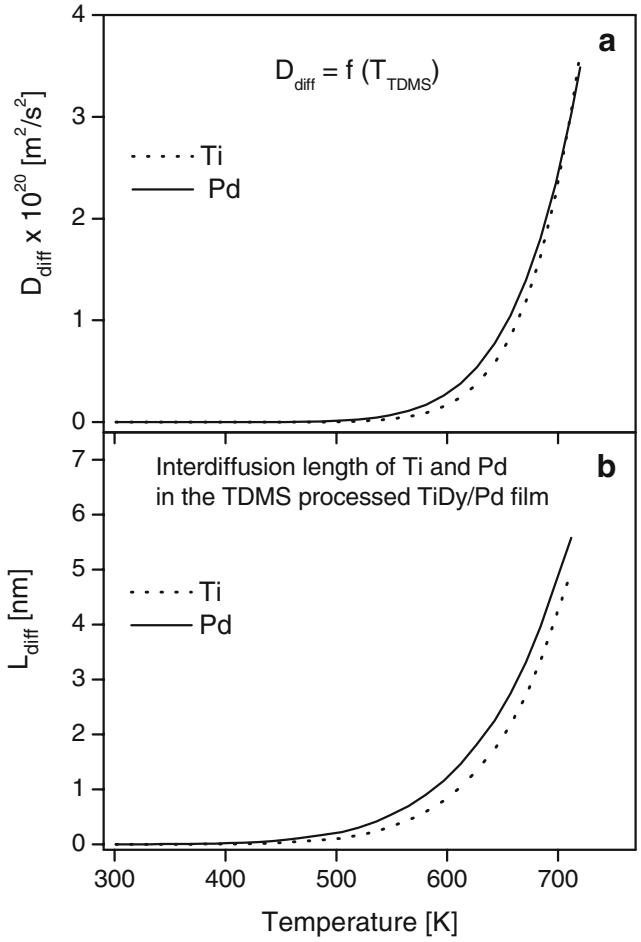

Fig. 5 **a** Diffusion coefficients (D_{diff}) of Ti and Pd in the Ti–Pd film for temperatures determined by the TDMS process. **b** A length of diffusion zone (L_{diff}) for Ti and Pd within the Pd–Ti interface of the TiD_y/Pd film determined for the following steps of the TDMS annealing. For a description of the L_{diff} value, see text

temperatures than in 10-nm-thick Ti films [4]. The ultrathin TiD_y layers exhibit much more disordered bulk morphology, which is dominated by amorphous areas in addition to the fine polycrystalline grains (8–12 nm) [4]. It therefore appears that Ti in this stage interacts easier with Pd than Ti from the stable crystalline TiD_2 phase, forming $PdTi_2$ and migrating faster within Pd layer.

A small concentration of Pd in a Si–Ti interlayer area of the film before TDMS (see Pd map in the left column of Fig. 3) is caused by intensive outgassing of the tungsten heater, used as Pd evaporator, prior to evaporation of Ti film.

XPS analysis

In order to analyze the chemical nature of the components formed within the surface region of the TDMS processed TiD_y/Pd films, both films, taken before and after TDMS, were investigated by means of angle-resolved (AR) XPS. Figure 6 shows a set of Ti 2p (a) and Pd 3d (b) detail XPS spectra recorded from the film before TDMS at an electron take-off angle of 90° (curves 1) and the TDMS processed film at 90° and 20° (curves 2 and 3 of Fig. 6, respectively). As can be seen, the XPS spectra do not reveal Ti in the surface and subsurface regions of the TiD_y/Pd film prior to the TDMS process (see line 1 in Fig. 6a). However, Ti is observed within the surface area after TDMS heating. ARXPS measurements reveal the relative atomic concentration ratio of Ti 2p/Pd 3d taken at 20° and 90° to be 2.52 and 0.79, respectively. This result confirms a significant enrichment of Ti within the surface area of the TDMS processed TiD_y/Pd film, which was shown earlier in the EF-TEM images (see, e.g., Figs. 3 and 4, right-hand-side columns).

The analysis of the Pd 3d XPS spectrum of the annealed TiD_y/Pd film (Fig. 6c) reveals the coexistence of three doublets in the Pd 3d spectra (Pd $3d_{5/2}$ peaks positioned at 335.0, 336.3, and 337.9 eV BE, and its corresponding Pd $3d_{3/2}$ peaks at 340.3, 341.6, and 343.2 eV BE, respectively), which can be ascribed to Pd, $PdTi_2$, and PdO_2 [16]. Identification of the $PdTi_2$ phase is based also on the observed 1.3 eV BE shift relative to pure Pd, which is in good agreement with the corresponding BE shift of 1.37 eV, reported by Bzowski and Sham [17] for $PdTi_2$. Our XPS results clearly show that the $PdTi_2$ intermetallic compound most likely is formed within the TiD_y/Pd film even after a short time of TDMS processing.

Correlation of TDMS spectra of deuterium with interdiffusion of Pd and Ti atoms in thin TiD_y/Pd films

In order to better elucidate the course of TDMS induced deuterium evolution from ultrathin TiD_y/Pd films, we have to recall some experimental data, which we reported lately

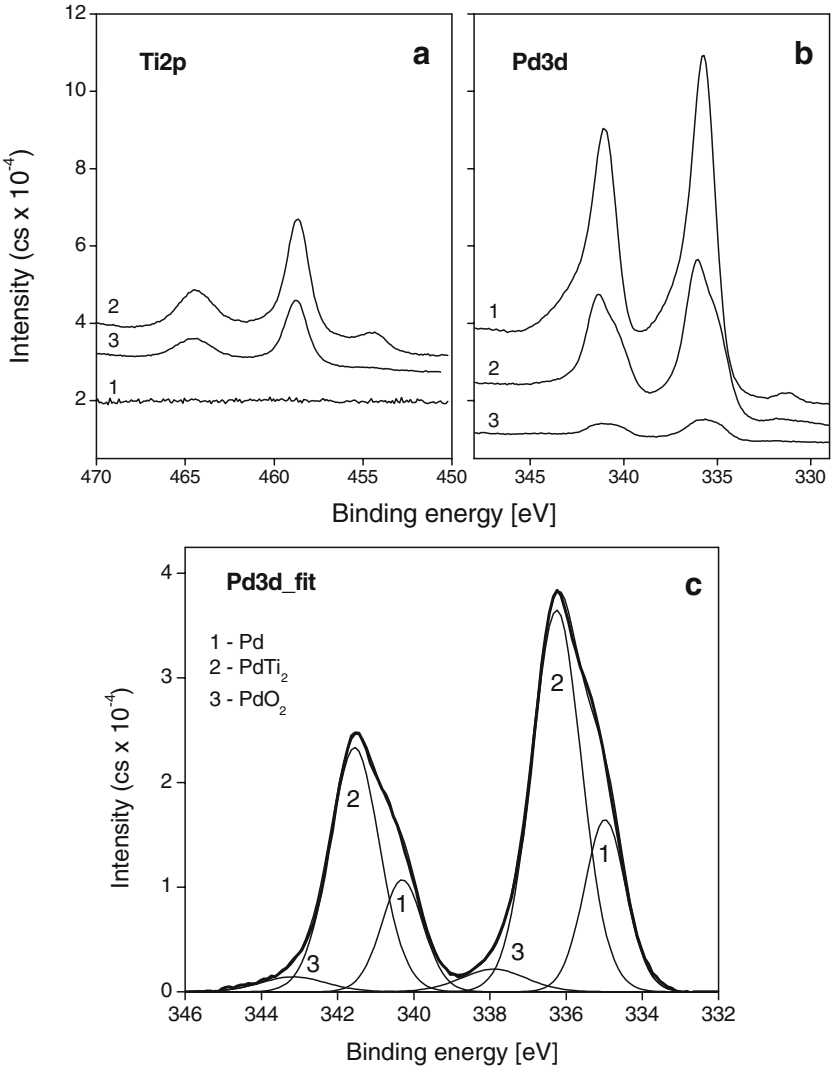

Fig. 6 Ti 2p (**a**) and Pd 3d (**b**) AR detail XPS spectra collected at 90° on the TiD_y/Pd film before and after TDMS processing (*lines 1* and *lines 2*, respectively) and at 20° on the TDMS processed film (*lines 3*). In **c**, the peak-fit analysis of the Pd 3d XPS spectrum, taken at 90° on the TDMS processed film, is shown

for the thermal decomposition of TiD_y films of similar thickness but not covered by a Pd layer [4]. TDMS heating induced decomposition of such films was found to proceed at low temperature (maximum peak temperature T_m about 500 K), and its kinetics was dominated by a low-energy desorption (E_D=0.61 eV) of deuterium from surface and subsurface areas of the Ti film. The origin of this process was discussed as an intermediate decomposition state towards recombinative desorption of molecular deuterium.

In view of these results, it is interesting to understand how a Pd layer, evaporated on top of a titanium deuterated film, can affect the deuterium evolution process. Firstly, we compared the diffusion parameters of deuterium in Ti, TiD_y, and Pd films as presented in Table 2. Table 2 shows that the diffusion coefficients of deuterium in Pd are higher than in Ti and $TiH_{1.98}$. Therefore, we can conclude that the diffusion transport of deuterium within the top Pd layer covering the TiD_y film should not affect the deuterium transport in the bulk of bi-layer film. As in the case of the TiD_y films, it is more likely that surface processes, which follow the deuterium transport within the bulk of the film, may play a decisive role as a rate limiting step in the TDMS kinetics. Structural and chemical analysis of ultrathin TiD_y/

Table 2 Selected data of diffusion parameters, E_{diff} and D_0, of hydrogen and deuterium in Ti, Pd, and TiD_y systems [18–23]

Diffusion system	D_0 [$m^2\ s^{-1}$]	E_{diff} [eV]	T [K]	Ref.
D in α-Ti	2.75×10^{-7}	0.43	873–1298	[18, 19]
D in $TiH_{1.74}$ powder	1.08×10^{-7}	0.60	620–800	[20]
D in $TiH_{1.98}$ powder	9.4×10^{-8}	0.67	690–820	[20]
D in Pd sphere	2.22×10^{-7}	0.22	298–1373	[21]
H in Pd film:135 nm thick	9.4×10^{-8}	0.38	280–330	[22]
H in Pd film: 22.5 nm thick	3.9×10^{-9}	0.38	280–330	[22]
H in Pd film	2.9×10^{-7}	0.23	300	[23]
H on Pd film surface	9.9×10^{-10}	0.43	Infinite	[21]

Pd films reveals a significant rearrangement in the surface and subsurface areas after TDMS. Both EFTEM and XPS analysis disclose a visible enrichment of Ti at the surface of the TDMS processed TiD_y/Pd film. This result is crucial for a correct interpretation of the associated TDMS spectra of deuterium released from an ultrathin TiD_y/Pd film. Evidently, the chemical composition at surface and subsurface regions is modified during TDMS processing, directly affecting the kinetics of desorption of D_2 and the course of TDMS deuterium spectra.

It is likely that within the low-temperature range of the TDMS process, between 300 and 500 K, the kinetics of deuterium evolution is dominated by recombinative desorption of D_2 from the Pd surface. Because deuterium desorption from the Pd film is expected to be realized at lower temperatures [24] than deuterium evolution from the TiD_y film [4], the maximum peak temperature T_{max} of the TDMS spectrum of deuterium from the TiD_y/Pd film is shifted to lower temperature as compared to the corresponding spectrum recorded from the TiD_y film (compare T_{max} of the corresponding TDMS spectra 1 and 2 in Fig. 1). As the TDMS heating temperature increases, the relative contribution of interdiffused Ti to the chemical surface composition is becoming more pronounced and will be dominant at the end of the TDMS process. As a result, the kinetics of deuterium evolution at temperatures higher than 500 K is becoming predominantly the result of desorption of D_2 from the Ti surface, inducing also a different course of the TDMS spectrum of deuterium in this temperature range. One can see in Fig. 1 that the asymmetric shape of the TDMS deuterium spectrum occurs at temperatures above 500 K, a region in which interdiffusion of Ti and Pd in the film becomes significant (compare the Pd and Ti interdiffusion analysis data presented in Fig. 5).

Summary and conclusions

The ultrathin TiD_y/Pd films can be considered as a useful material for deuterium storage purposes. TDMS spectra reveal deuterium evolution from such material within a temperature range of 350–600 K. It was found that the annealing of an ultrathin TiD_y/Pd film, performed under conditions determined by the TDMS process, leads to extensive film structure transformations. Both EFTEM and XPS analysis of the annealed film showed a visible enrichment of Ti at the top of the Pd film surface, providing a more accurate insight into the kinetics of deuterium evolution induced by TDMS annealing. The kinetics of this process is progressively changed during TDMS; at temperatures lower than 500 K, it is limited by recombinative desorption of deuterium from the Pd surface, and at temperatures higher than 500 K, the kinetics will get dominated by a time-dependent interdiffusion of Ti into the Pd surface.

References

1. Westlake DG, Satterthwaite CB, Weaver JH (1978) Phys. Today 31:32–39
2. Hirooka Y (1984) J Vac Sci Technol A 2:16–21
3. Kirchheim R, Fromm E, Wicke E (1989) (eds) Metal-hydrogen systems: Fundamentals and applications (Proceedings of the first international symposium combining “hydrogen in metals” and “metal hydrides” Stuttgart, 1988), R. Oldenburg Verlag, Munich
4. Lisowski W, Keim EG, Kaszkur Z, Smithers MA (2008) Appl Surface Sci 254:2629–2637
5. Lisowski W, Keim EG, van den Berg AHJ, Smithers MA (2006) Anal Bioanal Chem 385:700–707
6. Lisowski W, Keim EG, Kaszkur Z, van den Berg AHJ, Smithers MA (2007) Anal Bioanal Chem 389:1489–1498
7. Nowicka E, Duś R (1996) Langmuir 12:1520–1527
8. Checchetto R, Gratton LM, Miotello A, Tomasi A, Scardi P (1998) Phys Rev B 58:4130–4137
9. Lisowski W (1999) Vacuum 54:13–18
10. Duś R, Lisowski W, Nowicka E, Wolfram Z (1995) Surf Sci 322:285–292
11. Lisowski W, Keim EG, Smithers MA (2003) J Vac Sci Tech A 21:545–552
12. Lisowski W, Keim EG, Smithers M (2002) Appl Surf Sci 189:148–156
13. Briggs D Seah MP (1983) (eds) Practical surface analysis by auger and X-ray photoelectron spectroscopy. Wiley, Chichester
14. Behar M, Soares MR, Dyment F, Pérez RA, Balart S (2000) Phil Mag A 6:1319–1334
15. Tadayyon SM, Yoshinari O, Tanaka K (1993) Jpn J Appl Phys 32:3928–3932
16. Wagner CD, Naumkin AV, Kraut-Vass A, Allison JW, Powell CJ, Rumble JR Jr (2003) NIST Standard Reference Database 20, Version 3.4, Web Version: http://srdata.nist.gov/xps/
17. Bzowski A, Sham TK (1993) Phys Rev B 48:7836–7840
18. Naito S, Yamamoto M, Miyoshi T, Mabuchi M, Doi M, Kimura M (1996) J Chem Soc Faraday Trans 92:3407–3410
19. Naito S, Yamamoto M, Doi M, Kimura M (1998) J Electrochem Soc 145:2471–2475
20. Kaess U, Majer G, Stoll M, Peterson DT, Barnes RG (1997) J Alloys Compd 259:74–82
21. Powell GL, Kirkpatrick JR (1991) Phys Rev 43:6968–6976
22. Li Y, Cheng YT (1996) Int J Hydrogen Energy 21:281–291
23. Wicke E, Brodowsky H, Züchner H, in Alefeld G and Völkl J (1978) (eds), Hydrogen in metals II. Springer, New York, p. 73
24. Lisowski W, Duś R (1993) Appl Surface Sci 72:149–156